THE ASTROPHYSICAL JOURNAL, 412:160–172, 1993 July 20

THE DISTANCE TO THE LARGE MAGELLANIC CLOUD: CONSTRAINTS FROM CEPHEIDS IN LARGE MAGELLANIC CLOUD STAR CLUSTERS

GIANPAOLO BERTELLI[1]
National Council of Research, CNR-GNA, Italy, and Osservatorio Astronomico di Padova, Vicolo dell'Osservatorio 5, Padova I-35122, Italy
ALESSANDRO BRESSAN
Osservatorio Astronomico di Padova, Vicolo dell'Osservatorio 5, Padova I-35122, Italy
CESARE CHIOSI
Department of Astronomy, Universitá di Padova, Vicolo dell'Osservatorio 5, Padova I-35122, Italy
MARIO MATEO[2]
Carnegie Observatories, 813 Santa Barbara Street, Pasadena, CA 91101
AND
PETER R. WOOD
Mount Stromlo and Siding Springs Observatory, Private Bag, Weston Creek Post Office, ACT 2611, Australia
Received 1992 July 16; accepted 1993 January 29

ABSTRACT

We have used recent observational data for the Cepheids in the rich, young Large Magellanic Cloud clusters NGC 1866 and NGC 2031 to constrain the cluster distances with the mass-equivalency (ME) method. The basis of this approach is to fix the cluster distances by requiring the Cepheid evolutionary and pulsational masses to be equal. Using evolutionary models incorporating a mild amount of core and envelope overshooting along with recent pulsational models, we derive distance moduli of 18.51 ± 0.21 and 18.32 ± 0.20 for NGC 1866 and NGC 2031, respectively. The quoted errors are dominated by the uncertainties in the heavy element abundances of the clusters (assumed to be 0.3 dex for both clusters), with a smaller contribution due to the apparently intrinsic spread in the masses of the Cepheids in each cluster. For the ME method, we find that $\Delta(m - M)_0/\Delta Z_1 = 0.69$, where $Z_1 \equiv \log (Z/0.016)$. This result implies that the cluster distances can be determined to better than $\pm 5\%$ if the cluster abundances can be measured to better than about ± 0.15 dex. The distance moduli we derive for NGC 1866 and NGC 2031 are consistent with other recent values derived for the LMC, meaning that the models used in this analysis avoid the classical evolutionary/pulsational Cepheid mass discrepancy. The results of our analysis are based on models using the Los Alamos opacities; had we used models incorporating the new Livermore opacities instead, we estimate that the cluster distance moduli would be larger by *at most* 0.1 mag.

Subject headings: Cepheids — galaxies: distances and redshifts — Magellanic Clouds — open clusters and associations: individual (NGC 1866, 2031) — stars: oscillations

1. INTRODUCTION

In a recent paper, Chiosi et al. (1992, hereafter Paper I) estimated the distance to the LMC cluster NGC 2157 by comparing the evolutionary and pulsational masses of its three Cepheids (Mateo, Olszewski, & Madore 1990). One of the primary conclusions of this work was that the distance to NGC 2157 could be precisely constrained by insisting that these masses agree—an approach we shall refer to as the mass-equivalency (ME) method. Not surprisingly, the moduli derived in this manner depend on the details of the evolutionary models employed and on the adopted effective temperature-color transformations. For example, using evolutionary models based on classical semiconvective mixing (e.g., Lattanzio 1991; Castellani et al. 1989; Fagotto 1990) and transformed to the $V - (B-V)$ color-magnitude diagram with the "Yale" temperature-color transformations (Green et al. 1987), a true distance modulus of 19.02 ± 0.10 was determined for NGC 2157 (Paper I). In contrast, applying the same procedure with the Padova overshoot evolutionary models (Bertelli et al. 1990) and the so-called Padova temperature-color transformations (see Paper I and § 3 below) resulted in a true distance modulus of 18.47 ± 0.08 for the cluster and its three Cepheids. When additional constraints from the color-magnitude diagram of the cluster were considered, the smaller modulus was clearly preferable; moreover, the latter value is in good agreement with various recent independent estimates of the distance to the LMC (Feast & Walker 1987; Panagia et al. 1991). Thus, we concluded in Paper I that (1) the ME method was a promising way of estimating the distance of the LMC, and (2) overshoot models resolved the long-standing Cepheid mass discrepancy between pulsational and evolutionary masses. Because of current efforts to find and study Cepheids in other Magellanic Cloud clusters (e.g., Mateo et al. 1990; P. Wood & M. Bessell 1991, private communication), and the importance of these stars for calibration of the extragalactic distance scale (Mateo 1993, and references therein), it is important to understand how variations in relevant physical properties significantly effect the distance moduli derived with the ME method.

One possibly important parameter is the chemical composition. In our earlier analysis of NGC 2157 (Paper I), we assumed a single composition, $Z = 0.008$, for all models. This choice is consistent with numerous recent abundance studies of

[1] Fellow of the National Council of Research, CNR-GNA, Italy.
[2] Hubble Fellow.

young and intermediate-age objects in the LMC. For example, Feast (1988) reviewed numerous abundance estimates of young stars and nebulae in the LMC, finding average [Fe/H] values of -0.12 for field Cepheids, -0.20 for nonvariable AF supergiants, ≥ -0.4 from infrared photometry of individual stars in young clusters, and -0.26 for H II regions. More recently, Russell & Bessell (1989) found a mean [Fe/H] $= -0.3 \pm 0.2$ from high-dispersion spectra of F-type field supergiants in the LMC, while Russell & Dopita (1990) derived [Fe/H] $= -0.3 \pm 0.1$ for a sample of supernova remnants, and [M/H] $= -0.25 \pm 0.2$ for H II regions (where "M" refers to Ne, S, Cl, and Ar). Recent abundance estimates of young LMC clusters yield similar results: Olszewski et al. (1991) derive [Fe/H] $= -0.3 \pm 0.2$ for their sample of young clusters in the inner LMC, while Da Costa (1991) independently found a similar abundance range for LMC clusters younger than about 0.5 Gyr. In contrast, Reitermann et al. (1990) found [Fe/H] $= -0.8$ for one supergiant in the young LMC cluster NGC 1818. Thus, although most young objects in the LMC appear to have heavy element abundances near [Fe/H] $= -0.2 \pm 0.2$, the full range of present-day abundances in the LMC may be significantly larger than implied by this value.

The practical consequence of all this is that one must admit a sizeable uncertainty in the metallicity of any young LMC cluster lacking an independent abundance determination. What is the quantitative importance of this uncertainty for distance moduli derived using the ME method? The primary aim of this paper is to answer this question using the recent observations of Cepheids in the rich LMC clusters NGC 1866 (Welch et al. 1991) and NGC 2031 (Mateo, Olszewski, & Welch 1993). As will become apparent, the rich Cepheid populations in these clusters are very similar; thus, by combining the analysis of both we obtain an important check on the reliability of our final results.

In the following section, we summarize the relevant observational data for NGC 1866 and NGC 2031 used in our analysis. The pulsational masses of the Cepheids in both clusters are derived in § 3 using the results of recent pulsational models developed by Chiosi, Wood, & Capitanio (1993b; also Chiosi & Wood 1991, unpublished, as quoted by Chiosi 1991). We demonstrate how these pulsational mass estimates depend on the assumed distance modulus. In § 4, we derive the evolutionary masses of the Cepheids in NGC 1866 and NGC 2031 based on analyses of the color-magnitude diagrams of both clusters, while in § 5 we compare the pulsational and evolutionary mass estimates in order to derive the cluster distances. The models used in this paper are based on the Los Alamos radiative opacities (Huebner et al. 1977) supplemented by the molecular contribution in the outer layers (Bessell et al. 1989; Chiosi et al. 1993b); the models *do not* incorporate the newest Livermore opacities (Iglesias & Rogers 1991a, b; Rogers & Iglesias 1992). Thus, the distances we derive in this paper for NGC 1866 and NGC 2031 are not meant to be definitive; nevertheless, we note in § 5 that the quantitative effect of incorporating the new opacities on our results is probably not very large. In any case, our analysis should be suitable for our primary purpose to establish the sensitivity—in a *differential* sense—of the ME method to metallicity. We summarize the paper and our main conclusions in § 6.

2. SUMMARY OF THE OBSERVATIONAL DATA

The data for the Cepheids studied in this paper are taken from Welch et al. (1991) for NGC 1866 and from Mateo et al. (1991) for NGC 2031; the relevant results are listed in Table 1. For each star, the mean V-magnitudes of the variables correspond to intensity means of smooth curves fit to the phased

TABLE 1

PHOTOMETRIC PROPERTIES OF CEPHEIDS IN NGC 1866 AND NGC 2031[a]

Cluster	Star	Period (days)	log P	$\langle V \rangle$ (mag)	$\langle B-V \rangle$[b] (mag)	Notes
NGC 1866.....	HV 12197	3.14	0.497	16.08	0.59	
	HV 12198	3.52	0.547	15.93	0.64	
	HV 12199	2.64	0.422	16.27	0.58	
	HV 12200	2.73	0.435	16.13	0.56	
	HV 12202	3.10	0.492	16.05	0.62	spectroscopic binary
	HV 12203	2.95	0.470	16.10	0.61	
	HV 12204	3.44	0.536	15.68	0.50	RV nonmember
	V4	3.32	0.521	16.06	0.67	
	V8	2.01	0.303	16.15	0.61	overtone pulsator
NGC 2031.....	1	3.07	0.487	15.82	0.48	probable binary
	2	4.43	0.646	15.88	0.67	
	3	3.96	0.598	16.01	0.72	
	4	3.43	0.535	15.98	0.65	
	5	3.32	0.521	16.02	0.63	
	6	3.03	0.481	16.03	0.58	
	7	3.13	0.496	16.12	0.64	
	8	3.27	0.515	16.18	0.62	
	9	2.95	0.470	16.18	0.63	
	10	3.32	0.521	16.18	0.72	
	11	2.82	0.450	16.31	0.67	
	12	1.84	0.265	16.43	0.66	overtone pulsator
	13	3.20	0.505	16.00	0.57	
	14	2.97	0.473	16.17	0.62	

[a] These data are taken from Welch et al. 1991 for NGC 1866, and Mateo et al. 1993 for NGC 2031.

[b] The $(B-V)$ colors listed here for NGC 2031 equal the mean of the observed values of $\langle B \rangle - \langle V \rangle$ and $\langle B-V \rangle$ for each Cepheid.

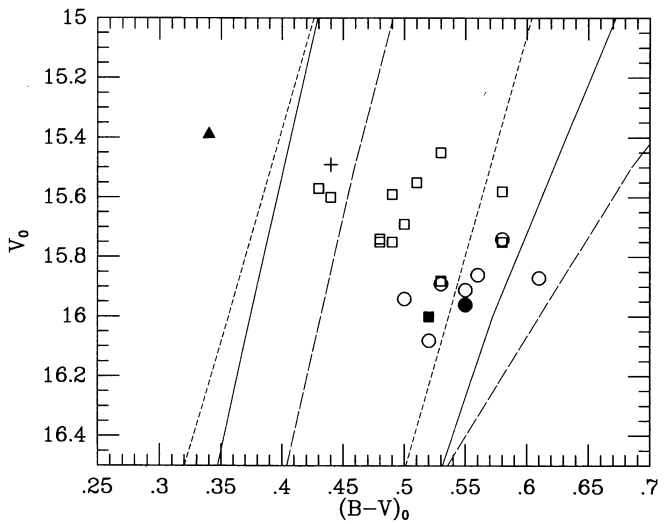

FIG. 1*a*

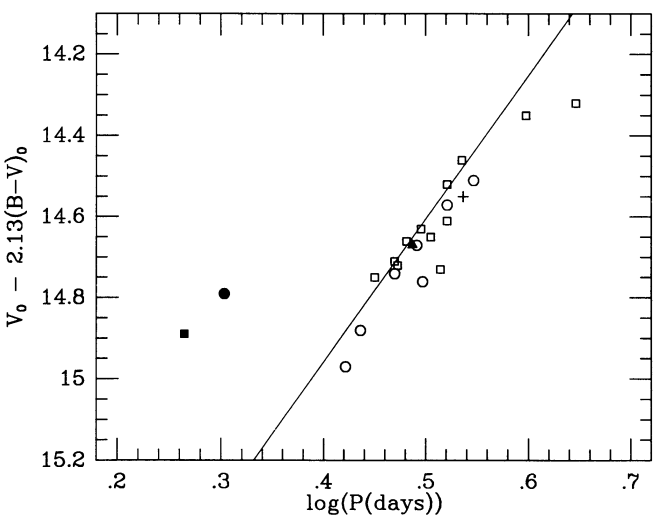

FIG. 1*c*

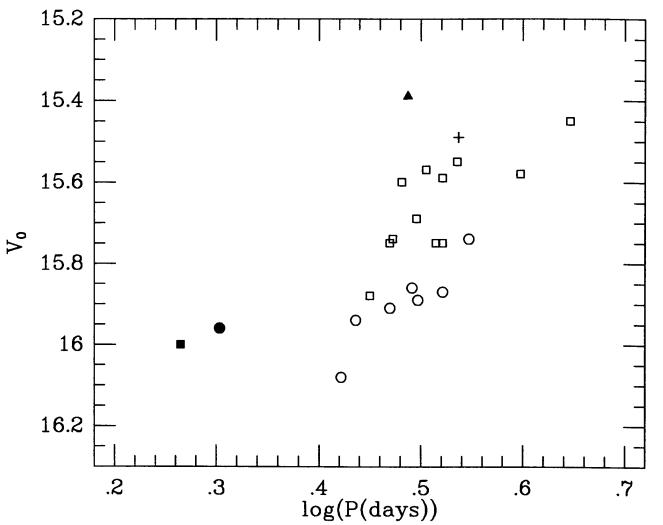

FIG. 1*b*

FIG. 1.—(*a*) Color-magnitude diagram of the Cepheids listed in Table 1. The circles represent the Cepheids in NGC 1866; the squares represent the Cepheids in NGC 2031. The filled circle and square show the locations of the overtone Cepheids in the two clusters, NGC 1866−V8 and NGC 2031−12, respectively. The filled triangle represents the probable binary Cepheid NGC 2031−1, while the cross shows the location of HV 12204, a radial velocity nonmember of NGC 1866. The solid lines represent the boundaries of the instability strip for fundamental pulsators with $Z = 0.008$ from the models of Chiosi et al. (1993b); the short-dashed line shows the boundaries for the first-overtone instability strip from the same models. The long-dashed line shows the boundaries of the instability strip empirically determined by Fernie (1990) for Galactic Cepheids. (*b*) Period-luminosity relation of the Cepheids listed in Table 1. The symbols have the same meaning as in Fig. 1*a*. (*c*) Period-luminosity-color relation for the Cepheids in Table 1. The $(B-V)$ coefficient was taken from Caldwell & Coulson (1986). The solid line shows the PLC relation for field Cepheids in the LMC derived by these authors. The symbols have the same meaning as in Fig. 1*a*.

light curves (see Welch et al. 1991 for details). The $(B-V)$ colors listed in Table 1 equal the means of $\langle B\rangle - \langle V\rangle$ and $\langle B-V\rangle$ for each Cepheid. Fernie (1990) noted that the former index is a preferable measure of the effective temperature of Cepheids; however, for low-amplitude, short-period variables such as those in NGC 1866 and NGC 2031, the two indices are essentially identical. We assume that the random errors in the V-magnitudes and $(B-V)$ colors are 0.02 and 0.03 mag, respectively. Because of the generally complete phase coverage for the Cepheids used in this study, these error estimates are likely to be conservative.

NGC 1866 and NGC 2031 are both exceptionally rich in Cepheids. Over 20 are known in NGC 1866 (Welch et al. 1991); nine of these have sufficiently precise light curves and periods to be used in our analysis. Although NGC 2031 contains slightly fewer Cepheids (14, all of which have well-determined light curves and periods), it contains 70% more Cepheids per unit luminosity than NGC 1866. In this paper, we adopt the color excesses assigned by the original studies of the Cepheids: for NGC 1866, $E(B-V) = 0.06 \pm 0.02$ mag, while for NGC 2031, $E(B-V) = 0.14 \pm 0.02$ mag. These reddenings have been derived (in the case of NGC 2031) from the mean $(B-V)$ and $(V-I)$ colors of the Ceopheids themselves (Dean, Warren, & Cousins 1978; Mateo et al. 1993), and from the color of the upper main sequences of both clusters. Throughout this paper we assume $A_V = 3.1E(B-V)$; color excesses and extinctions in other bands have been determined using the mean extinction curve given by Cardelli et al. (1989).

The dereddened color-magnitude diagram of the program Cepheids is illustrated in Figure 1*a*. Also shown are the empirical edges of instability strip from Fernie (1990) for Galactic Cepheids, and the theoretical instability strip boundaries from Chiosi et al. (1993b). The theoretical boundaries correspond to $Z = 0.008$ and assume a mass-luminosity relation taken from overshoot evolutionary models transformed to the observational plane using the Padova transformations (see Paper I). The fact that the stars plotted in Figure 1*a* are predominantly located on the red side of the instability strip implies that their evolutionary paths barely penetrate the strip from the right. Because the evolution at the blue end of the loops that carry stars into the instability strip is relatively slow (e.g., Becker & Mathews 1983), this also helps explain why these clusters contain so many Cepheids (Becker & Mathews 1983). Figure 1*b* shows the location of the NGC 1866 and NGC 2031 Cepheids in the period-luminosity (PL) plane, while one version of the period-luminosity-color (PLC) relation for these stars is shown in Figure 1*c*. It is evident from Figures 1*b* and 1*c* that two of the Cepheids in the present sample, V8 in NGC

1866 and 12 in NGC 2031, are pulsating in the first overtone. As expected for this pulsation mode (Iben & Tuggle 1975), the ratios of the observed periods of these two stars divided by their fundamental-mode periods corresponding to the PLC relation (Caldwell & Coulson 1986) is approximately 0.7. In contrast to the two overtone pulsators in NGC 2157 (Mateo et al. 1990; Paper I), the overtone Cepheids in NGC 1866 and NGC 2031 are not the bluest Cepheids of their respective samples. The slight offsets of the individual PLC relations of NGC 1866 and NGC 2031 are consistent with the tilted-disk model of the LMC proposed by Caldwell & Coulson (1986) based on an analysis of LMC field Cepheids. The primary implication of this interpretation is that NGC 1866 is slightly further away (by about 3% or 0.06 mag) than NGC 2031.

The period distributions of the Cepheids in NGC 1866 and NGC 2031 are shown in Figure 2 to be very similar. Not surprisingly, the mean periods of the fundamental pulsators in each cluster are also nearly equal: for NGC 1866 $\langle P_f \rangle = 3.09$ days, while for NGC 2031 $\langle P_f \rangle = 3.34$ days. One of the Cepheids in NGC 1866 (HV 12204) was shown by Welch et al. (1991) to be a nonmember based on its radial velocity; it has been excluded from our analysis. Likewise, Cepheid NGC 2031 − 1 was discarded because its unusually blue colors imply that it is a member of an unresolved binary (Mateo et al. 1991). Although radial velocity measurements of HV 12202 in NGC 1866 show it to be a spectroscopic binary (Welch et al. 1991), we have kept it in our sample because it exhibits no unusual photometric properties that belie its binary nature.

To derive evolutionary masses of the Cepheids in the two clusters, we will adopt color-magnitude diagrams (CMDs) based on the photometry of Chiosi et al. (1989a, b) for NGC 1866, and of Mateo et al. (1993) for NGC 2031. The photometric results of Chiosi et al. (1989a, b) for NGC 1866 have been shifted by +0.11 mag in V and −0.025 in $(B-V)$ to account for the systematic photometric errors noted by Welch et al. (1991). The adopted CMDs of both clusters are shown in Figure 3.

Rough estimates of the chemical abundances of NGC 1866 and NGC 2031 have been derived from the BVI_C colors of the Cepheids as described by Caldwell & Coulson (1985). Feast (1989) applied this method using the photometry of Walker (1987) for NGC 1866 and found a mean abundance of [Fe/H] = −0.1 ± 0.2. Similarly, Mateo et al. (1993) derive [Fe/H] = −0.4 ± 0.2 for the NGC 2031 Cepheids. Because this method of deriving abundances is very sensitive to the adopted reddening and the precision of the atmospheric models employed to calibrate the technique, these internal errors are certainly optimistic. In this paper we shall therefore adopt the following abundance estimates: $[Fe/H]_{NGC1866} = -0.1 \pm 0.3$, and $[Fe/H]_{NGC2031} = -0.4 \pm 0.3$. These uncertainties are consistent with the range of abundances observed among young objects in the LMC (see § 1). The pertinent global properties of NGC 1866 and NGC 2031 are summarized in Table 2.

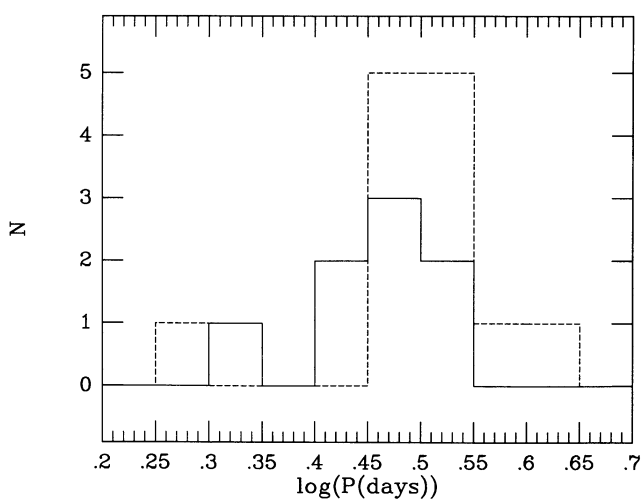

FIG. 2.—Period distribution of the Cepheids in NGC 1866 (*solid line*) and NGC 2031 (*dashed line*).

3. THE PULSATIONAL MASSES OF THE CEPHEIDS IN NGC 1866 AND NGC 2031

The pulsational masses of the Cepheids in NGC 1866 and NGC 2031 were derived using the procedure described in Paper I for the Cepheids in NGC 2157. For convenience we summarize the important points here.

The models used to derive the Cepheid pulsational masses were recently computed by Chiosi et al. (1993b) using an improved treatment of the opacity and outer convection zones compared to the earlier models of Iben & Tuggle (1972a, b, 1975). Cepheid models were computed for a wide range of masses, temperatures, and luminosities and the edges of the instability strip were parameterized as a function of these properties and the pulsation period. The blue edge of the instability strip was always well-defined as the point where the growth rate of pulsational instabilities becomes positive. We follow Chiosi et al. (1993b), who defined the red edge of the instability strip as the point corresponding to the maximum of the pulsation growth rates. This is a conservative choice in that unstable models are found at lower temperatures. The precise location of the red edge is difficult to determine because of the increased coupling of pulsation and convection as $T_{\rm eff}$ decreases; thus, the instability strip is likely to be even wider than assumed by Chiosi et al. (1993b). Three mass-luminosity (ML) relations were considered by Chiosi et al. (1993b) to construct the PL, and PLC relations from their models. These ML relations were obtained from models incorporating only semiconvection, and from models with mild and extreme core overshooting ($\Lambda = 0.5$ and 1.0, respectively; see Paper I for details). It is very important to stress that the mass-period-luminosity-color (MPLC) relation of Chiosi et al. (1993b) which we use in our analysis to determine the pulsational masses of the Cepheids in NGC 1866 and NGC 2031 does *not* depend on the underlying ML relation, only on the properties of the pulsation models.

Two different color-temperature and bolometric correction scales were discussed in Paper I; the so-called "Padova" and "Yale" scales. For a variety of reasons, we concluded in Paper I that the Padova conversion scales were most consistent with the data for NGC 2157 and its Cepheids; therefore, we will adopt the Padova transformation throughout this paper. In any case, the relative sensitivity of the ME method on metal-

TABLE 2

GLOBAL PROPERTIES OF NGC 1866 AND NGC 2031

Cluster	N_{Ceph}	$E(B-V)$	A_V	[Fe/H]
NGC 1866.....	$\gtrsim 20$	0.06	0.19	-0.1 ± 0.3
NGC 2031.....	14	0.14	0.43	-0.4 ± 0.3

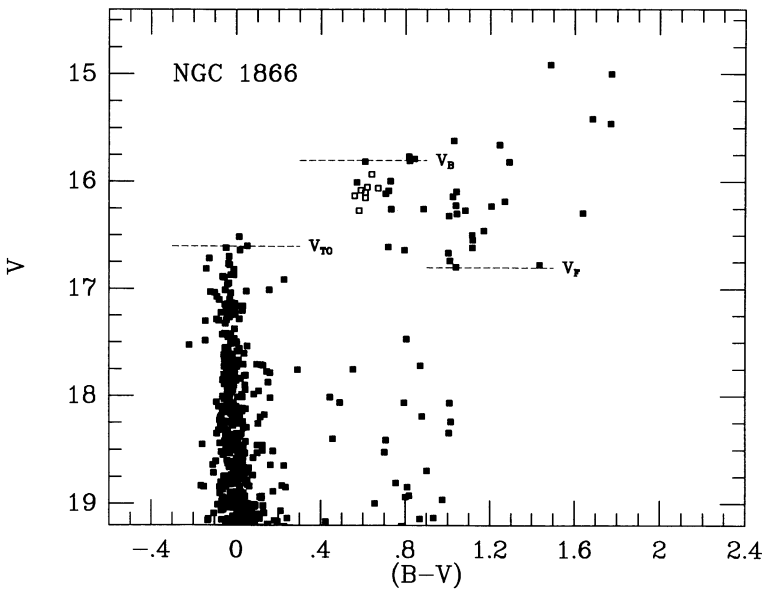

FIG. 3*a*

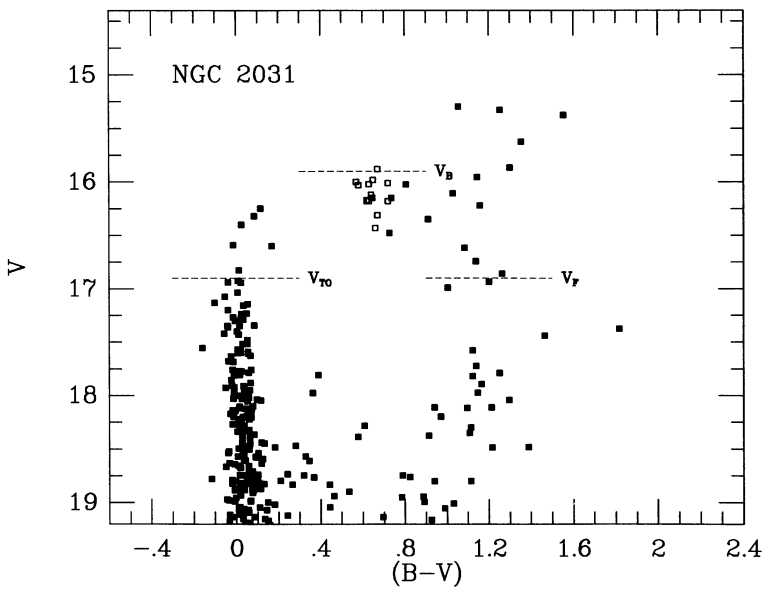

FIG. 3*b*

FIG. 3.—(*a*) Color-magnitude diagram of NGC 1866 for stars in an annulus with inner and outer radii of 31″ and 58″, respectively. These data are taken from Chiosi et al. (1989a, b). The three short horizontal lines illustrate the locations of the fiducial magnitudes used to derive the evolutionary masses of the Cepheids in § 4 of the text. The open squares show the locations of the Cepheids. (*b*) Same as Fig. 3*a*, but for an annulus with inner and outer radii of 12″ and 66″ centered on NGC 2031. The lines and symbols have the same meaning as in Fig. 3*a*.

licity is not a strong function of the adopted evolutionary models or conversion scale.

Two slightly different MPLC relations are used in the present analysis. The first one was developed by Chiosi & Wood (1991, unpublished) and was adopted in Paper I to determine the pulsational masses of the Cepheid stars of NGC 2157. This relation is

$$\log (M_p/M_\odot) = A + B \log (P) + C(B-V)_0 + DM_{V,0} , \quad (1)$$

where M_p is the pulsational mass, and P, $(B-V)_0$, and $M_{V,0}$ are the period (in days), the dereddened $(B-V)$ color, and the absolute V-magnitude corrected for extinction, respectively. The values of these coefficients corresponding to $Z = 0.004$, 0.008, and 0.016 are listed in Table 3 (all for $Y = 0.25$) for both the fundamental and first overtone pulsation modes.

The second MPLC relation was obtained by Chiosi et al. (1993b). It differs from the previous one for the inclusion of a quadratic term in $(B-V)$ that was introduced to parameterize the theoretical results more precisely. The relation is

$$\log (P_0) + 0.691 \log (M_p/M_\odot) = -(0.549 + 0.007Z_1) - (0.335 - 0.009Z_1)M_V + (1.107 + 0.798Z_1^2)(B-V) - (0.063 + 0.677Z_1^2)(B-V)^2 \quad (2)$$

TABLE 3

COEFFICIENTS OF THE MPLC RELATION[a]

		FUNDAMENTAL MODE				FIRST OVERTONE			
Y	Z	A	B	C	D	A	B	C	D
0.25	0.016	−0.61	−1.31	1.29	−0.45	−0.93	−1.58	1.43	−0.51
0.25	0.008	−0.64	−1.37	1.37	−0.47	−0.82	−1.48	1.37	−0.48
0.25	0.004	−0.68	−1.43	1.48	−0.48	−0.80	−1.46	1.38	−0.48

[a] From Chiosi & Wood 1991, unpublished. The form of the MPLC and the definition of the coefficients is given in eq. (1) of the text.

for the fundamental mode, and

$$\log (P_1) + 0.527 \log (M_p/M_\odot) = -(0.749 + 0.04Z_1) - (0.310 - 0.006Z_1)M_V + (1.294 + 0.904Z_1^2)(B-V) - (0.307 + 0.938Z_1^2)(B-V)^2 \quad (3)$$

for the first overtone. All the symbols have their usual meaning, and $Z_1 \equiv \log (Z/0.016)$.

Mass estimates based on equation (1) for the Cepheids in NGC 1866 and NGC 2031 are listed in Table 4A for three different values of the true distance moduli of the clusters. The typical error in M_p for a given star and assumed distance modulus is approximately 10%. The photometric errors (described in § 2) contribute most of the uncertainties in the masses; the remainder can be attributed to uncertainties in the theoretical models used to construct the adopted MPLC relation. The corresponding mass estimates based on equations (2) and (3) are given in Table 4B. From comparing the entries of Tables 4A and 4B it is evident that both relations yield similar values although equations (2) and (3) tend to predict systematically slightly higher masses.

The strong dependence of M_p on distance apparent in Table 4 is illustrated in Figure 4 for the three abundances. Only results based on the MPLC relations given in equations (2) and (3) are plotted in Figure 4; similar diagrams can be constructed using the older MPLC relation (eq. [1]). For a given distance modulus and metallicity, the spread in M_p evident in Figure 4 equals the *full range* of pulsational masses for the Cepheids in each cluster. Note that this spread in individual Cepheid masses is somewhat larger than expected from the formal errors of 10% per star. This may indicate an intrinsic mass range among the Cepheids in each cluster caused by different amounts of mass loss among their progenitors or from a small age dispersion ($\lesssim 10^7$ yr; e.g., see Carney, Janes, & Flower 1985, and Paper I) within the clusters. It is clear from Table 4 and Figure 4 that the pulsational masses are moderately sensitive to changes in metallicity in the sense that lower abundances imply larger masses at a given assumed distance modulus.

4. THE EVOLUTIONARY MASSES OF THE CEPHEIDS IN NGC 1866 AND NGC 2031

As in § 3, the analysis in this section closely follows that of Paper I. The most important difference is that in this case the photometric results for NGC 1866 nor NGC 2031 are not sufficiently deep to provide an estimate of the distances to the clusters via main-sequence fits. Consequently, in order to estimate the cluster ages we have defined a set of fiducial magnitudes characterizing the luminosities of the more evolved stars in NGC 1866 and NGC 2031. These fiducial magnitudes are marked in the CM diagrams of NGC 1866 and NGC 2031 shown in Figure 3, and are defined as follows: V_{TO} is the luminosity of the upper termination point of the main sequence; V_F is the faint boundary of the evolved stars in the clusters; and V_B is the bright limit of the bluest evolved stars in the cluster. Observationally, these fiducial magnitudes are reasonably well-determined; we shall assume an uncertainty of ± 0.2 mag for each in our analysis. The adopted values for V_{TO}, V_F, and V_B for each cluster are listed in Table 5. The most important advantage of using fiducial magnitudes is that we can estimate

TABLE 4A

CEPHEID PULSATIONAL MASSES AS A FUNCTION OF DISTANCE AND METALLICITY[a]

			$(m-M)_0$ $Z=0.004$			$(m-M)_0$ $Z=0.008$			$(m-M)_0$ $Z=0.016$		
CLUSTER	STAR	MODE[b]	18.2	18.5	18.8	18.2	18.5	18.8	18.2	18.5	18.8
NGC 1866.....	HV 12197	F	3.8	5.3	7.4	3.1	4.3	5.9	2.9	3.9	5.4
	HV 12198	F	4.5	6.3	8.8	3.6	5.0	7.0	3.4	4.6	6.3
	HV 12199	F	3.8	5.3	7.4	3.1	4.3	5.9	2.9	3.9	5.4
	HV 12200	F	4.0	5.6	7.7	3.2	4.5	6.2	3.0	4.1	5.6
	HV 12202	F	4.4	6.2	8.7	3.6	4.9	6.8	3.3	4.5	6.2
	HV 12203	F	4.4	6.1	8.5	3.5	4.8	6.7	3.3	4.4	6.1
	V4	F	4.7	6.6	9.2	3.8	5.2	7.2	3.5	4.7	6.5
	V8	O	3.9	5.4	7.6	3.6	5.0	7.0	3.3	4.7	6.7
NGC 2031.....	2	F	3.8	5.3	7.4	3.1	4.3	6.0	2.9	4.0	5.5
	3	F	4.6	6.4	8.9	3.7	5.1	7.1	3.4	4.7	6.4
	4	F	4.6	6.4	8.9	3.7	5.2	7.2	3.5	4.7	6.5
	5	F	4.3	6.0	8.3	3.5	4.9	6.7	3.3	4.5	6.1
	6	F	4.1	5.7	7.9	3.4	4.7	6.4	3.2	4.3	5.9
	7	F	4.3	6.0	8.4	3.5	4.9	6.8	3.3	4.5	6.1
	8	F	3.5	4.9	6.9	2.9	4.1	5.6	2.8	3.8	5.1
	9	F	4.2	5.9	8.2	3.5	4.8	6.7	3.2	4.4	6.0
	10	F	4.9	6.8	9.5	3.9	5.4	7.5	3.6	5.0	6.8
	11	F	4.5	6.3	8.7	3.6	5.0	7.0	3.4	4.6	6.3
	12	O	3.8	5.4	7.5	3.6	5.0	7.0	3.3	4.7	6.7
	13	F	3.8	5.2	7.3	3.1	4.3	6.0	2.9	4.0	5.5
	14	F	4.1	5.7	8.0	3.4	4.7	6.5	3.2	4.3	5.9

[a] As described in § 5, the typical error of these masses is 10%; all masses are in solar units. The results listed in this table are based on eq. (1).
[b] "F" refers to the fundamental mode; "O" refers to the first overtone.

TABLE 4B

CEPHEID PULSATIONAL MASSES AS A FUNCTION OF DISTANCE AND METALLICITY[a]

CLUSTER	STAR	MODE[b]	$(m-M)_0$ $Z=0.004$			$(m-M)_0$ $Z=0.08$			$(m-M)_0$ $Z=0.016$		
			18.2	18.5	18.8	18.2	18.5	18.8	18.2	18.5	18.8
NGC 1866.....	HV 12197	F	3.7	5.3	7.4	3.0	4.1	5.8	2.7	3.7	5.2
	HV 12198	F	4.5	6.3	8.9	3.5	4.9	6.9	3.2	4.5	6.2
	HV 12199	F	3.7	5.3	7.4	3.0	4.1	5.8	2.7	3.8	5.3
	HV 12200	F	3.9	5.5	7.7	3.1	4.3	6.1	2.8	3.9	5.5
	HV 12202	F	4.4	6.2	8.7	3.5	4.8	6.8	3.1	4.4	6.1
	HV 12203	F	4.3	6.1	8.5	3.4	4.7	6.7	3.1	4.3	6.0
	V4	F	4.7	6.6	9.3	3.7	5.2	7.2	3.3	4.7	6.5
	V8	O	4.6	6.9	10.5	3.5	5.2	7.9	3.1	4.7	7.0
NGC 2031.....	2	F	3.8	5.3	7.5	2.9	4.1	5.8	2.7	3.7	5.2
	3	F	4.6	6.4	9.0	3.6	5.0	7.0	3.2	4.5	6.3
	4	F	4.5	6.4	9.0	3.6	5.0	7.0	3.2	4.5	6.3
	5	F	4.2	5.9	8.3	3.3	4.7	6.5	3.0	4.2	5.9
	6	F	4.0	5.6	7.8	3.1	4.4	6.2	2.8	4.0	5.6
	7	F	4.2	6.0	8.4	3.3	4.7	6.6	3.0	4.2	5.9
	8	F	3.5	4.9	6.8	2.7	3.8	5.4	2.5	3.5	4.8
	9	F	4.2	5.9	8.2	3.3	4.6	6.5	3.0	4.2	5.8
	10	F	4.8	6.8	9.6	3.8	5.3	7.5	3.4	4.8	6.7
	11	F	4.4	6.2	8.8	3.5	4.9	6.9	3.2	4.4	6.2
	12	O	4.5	6.8	10.4	3.4	5.2	7.8	3.1	4.6	6.9
	13	F	3.8	5.1	7.2	2.9	4.1	5.7	2.6	3.7	5.1
	14	F	4.0	5.7	8.0	3.2	4.5	6.3	2.9	4.0	5.6

[a] As described in § 5, the typical error of these masses is 10%; all masses are in solar units. The results listed in this table are based on eqs. (2) and (3).

[b] "F" refers to the fundamental mode; "O" refers to the first overtone.

the cluster ages and distances using primarily luminosity information, thus avoiding any strong dependence on theoretically determined colors. The latter are notoriously difficult to calculate reliably for evolved stars executing blue loops (Stothers & Chin 1991; Chiosi, Bertelli, & Bressan 1993a).

From Figure 3*b* it is evident that the estimate of V_{TO} for NGC 2031 is complicated by the presence of five brighter stars of comparable color to the main sequence. Owing to the low total luminosity of this cluster compared to NGC 1866, the annulus used to select stars for the NGC 2031 CM diagram extended closer to the cluster center in order to minimize field star contamination. Consequently, the typical crowding for measurable stars is actually more severe for NGC 2031 Cepheids than for NGC 1866. We shall show that the adopted value of V_{TO} for NGC 2031 is consistent with the two other fiducial magnitudes and that the bright stars are very likely physical or visual binaries.

Theoretical estimates of the values of the fiducial magnitudes

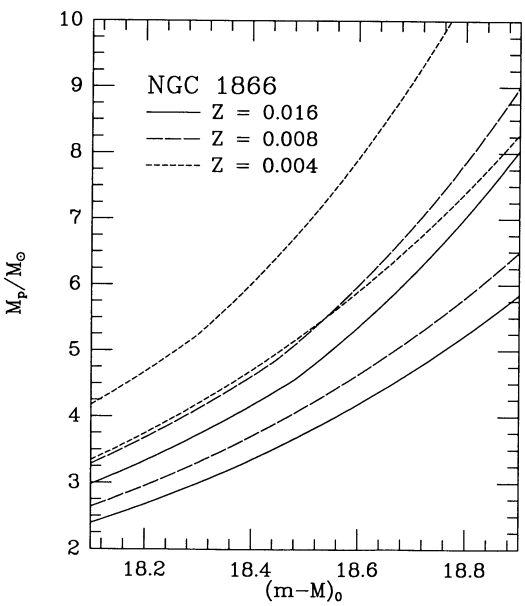

FIG. 4*a*

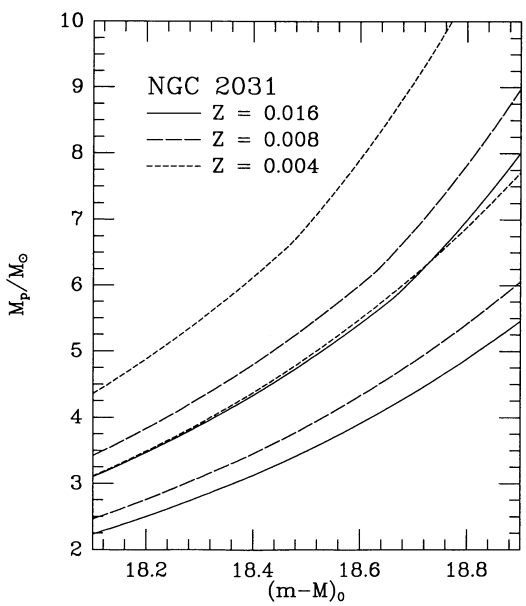

FIG. 4*b*

FIG. 4.—Variation of the pulsational mass of the Cepheids in NGC 1866 as a function of metallicity and assumed true distance modulus. (*b*) Same, for NGC 2031.

TABLE 5

MAIN-SEQUENCE TURNOFF AND BLUE LOOP FIDUCIAL MAGNITUDES[a]

	NGC 1866		NGC 2031	
PARAMETER[b]	Observed	Dereddened	Observed	Dereddened
V_{TO}	16.6	16.4	16.9	16.5
V_F	16.8	16.6	16.9	16.5
V_B	15.8	15.6	15.9	15.5

[a] See Fig. 3 for the definition of the parameters listed in this table.

[b] The typical uncertainty of the values listed in this table is ± 0.2 mag; see § 4 for further discussion.

V_{TO}, V_F, and V_B were determined from synthetic CM diagrams for NGC 1866 and NGC 2031 constructed in a manner analogous to Paper I using the models of Alongi et al. (1993). These models were calculated using mild core and envelope overshooting. The basic parameters determined from the models included the cluster age, and the evolutionary masses of its Cepheids, M_e, corresponding to this age.

To illustrate our procedure, Figure 5 shows two synthetic CM diagrams constrained to have a comparable number of evolved stars as observed in NGC 1866; the model results correspond to clusters with ages of 0.7×10^8 and 2.5×10^8 yr, $Z = 0.008$ and internal age dispersions of 0.05×10^8 yr. The

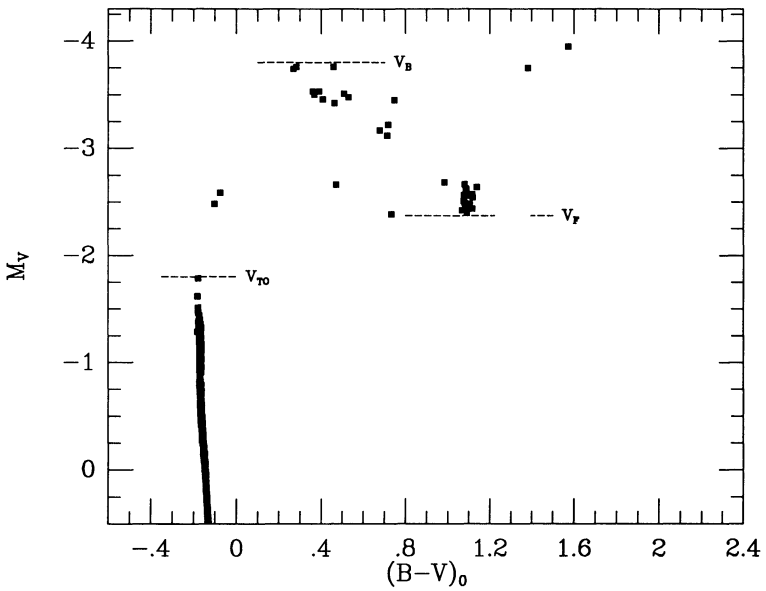

FIG. 5a

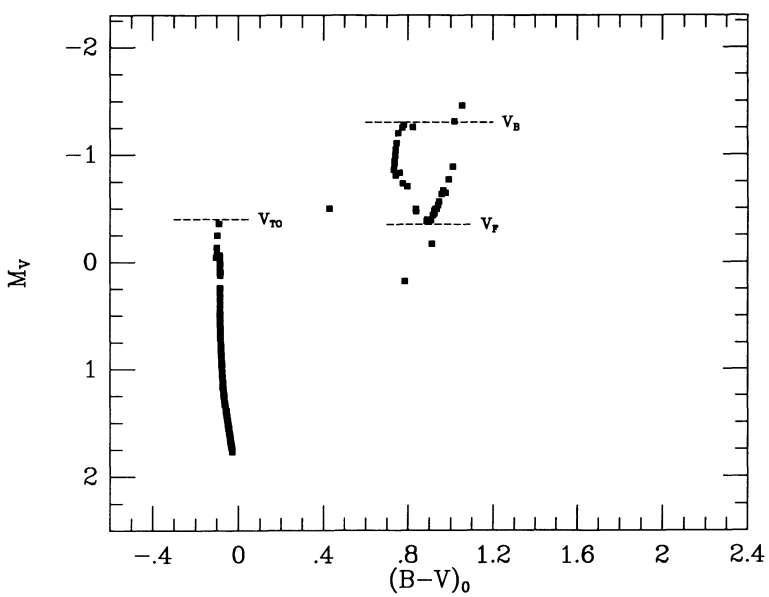

FIG. 5b

FIG. 5.—(*a*) Synthetic color-magnitude diagram based on overshoot models with $\Lambda = 0.5$ and corresponding to a cluster with an age of 0.7×10^8 yr, an internal age spread of 0.05×10^8 yr, and $Z = 0.008$ without binaries. The fiducial magnitudes defined in § 4 and Fig. 3 are also marked. (*b*) Same as Fig. 5*a* but for a synthetic cluster of age 2.5×10^8 yr.

same fiducial magnitudes derived from the observed CM diagram (Fig. 3*a*) are marked for the synthetic "data" in Figure 5. It is apparent that the separation of the faintest and brightest evolved stars in the younger simulated cluster (1.4 mag) is considerably larger than observed (1.0 mag), while for the older simulated cluster, the separation is too small (0.6 mag). In addition, it is clear that the relative values of V_{TO} and V_F in the younger simulation (Fig. 5*a*) do not reproduce the observations. Although the older simulated cluster (Fig. 5*b*) reproduces the *relative* values of V_{TO} and V_F adequately, the predicted turnoff magnitude is implausibly faint unless the true LMC distance modulus is smaller than 17.5! These discrepancies are characteristic of all relevant evolutionary models, not just those used in this paper (e.g., see Maeder & Meynet 1988; Chiosi et al. 1989a, b; Vallenari et al. 1993).

In Figure 6 we show a simulation for a cluster with an age of 1.2×10^8 yr, an age spread of 0.05×10^8 yr, $Z = 0.008$, and a population where 25% of the stars are in binaries with mass ratios equally distributed between 0.7 and 1.2. It is clear that while V_F and V_B do not significantly differ from the no-binary case, V_{TO} is brighter than before due to the presence of the binaries. The resulting relative values of V_{TO} and V_F are in better agreement with the observations (Table 5). Our goal in this paper is not to argue for or against the presence of binaries in NGC 1866 and NGC 2031; rather, the simulations shown in Figures 5 and 6 are meant to illustrate the extremes of the plausible model results that have been "fit" to the observed CM diagrams. Of course, two of the 22 cluster Cepheids in our sample *are* binaries (see Table 1; HV 12204 in NGC 1866 is not considered). Because Cepheids are highly evolved supergiants, this observed frequency of $\sim 10\%$ is consistent with a higher overall binary frequency on the main sequence.

Using a complete set of such simulated CM diagrams for three metallicities ($Z = 0.001$, 0.008, and 0.020), we have determined the absolute magnitudes of the fiducial magnitudes over a wide range of assumed ages (0.5×10^8 to 2.0×10^8 yr) and assumed true distance moduli (18.1 to 18.9). Comparison with the models then yielded the cluster ages and Cepheids masses. In order to match the metallicities used in the pulsational models, we have interpolated within the set of evolutionary models to derive mass and age estimates corresponding to $Z = 0.004$ and 0.016. Because of the special sensitivity of V_{TO} on the presence of binaries, the final age and evolutionary mass estimates were determined by allotting the results based on V_{TO} half the weight of the results derived from the other two fiducial magnitudes. A subset of these age and mass estimates are listed in Table 6. The variation of the evolutionary mass, M_e, as a function of true distance modulus is illustrated in Figure 7 for both clusters using the models incorporating binaries. In contrast to the pulsational masses, M_e decreases with decreasing metallicity.

Three points should be emphasized regarding the evolutionary masses derived above. First, the range of acceptable evolutionary masses at a given distance modulus and for a given metallicity (Fig. 7) reflects the quality of the "fit" of the synthetic CM diagrams compared to the observed diagrams. Thus, the large uncertainties quoted for the evolutionary masses (M_e) for the case $Z = 0.004$ really means that none of the models with this metallicity adequately fit the data (see Table 6). Second, the results based on cluster simulations without binaries *always* resulted in significantly poorer fits to the observed fiducial magnitudes: at a given modulus and metallicity, the range in M_e is typically larger by 20%–30% compared to the simulations with binaries. However, the *mean* ages and masses do not differ significantly whether or not binaries are included in the models. Finally, the brightest stars located above the adopted main-sequence termination point in NGC 2031 (Fig. 3*b*) cannot be understood using the adopted evolutionary models. Specifically, even for models with 100% binaries, V_{TO} is never 0.5 mag brighter than V_F as required if those stars represent the true termination point of the NGC 2031 main-sequence. Thus, it is likely that the brightest blue stars in the NGC 2031 CM diagram result from the severe crowding near the cluster center. However, if this is not the

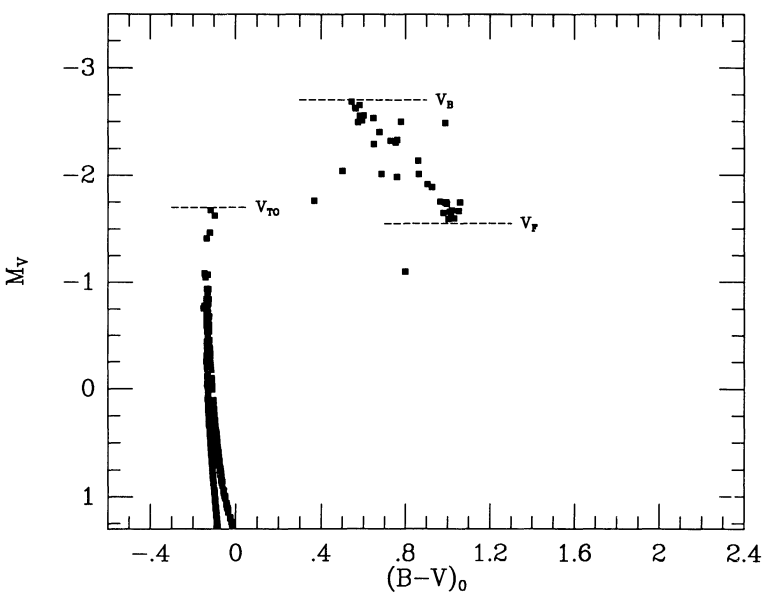

FIG. 6.—Synthetic color-magnitude diagram based on overshoot models with $\Lambda = 0.5$ and corresponding to a cluster with an age of 1.2×10^8 yr, an internal age spread of 0.05×10^8 yr, and $Z = 0.008$. Binaries with mass ratios uniformly distributed between 0.7 and 1.2 were assumed to make up 25% of the total population of stars in this "cluster."

TABLE 6

AGES AND CEPHEID MASSES OF NGC 1866 AND NGC 2031[a]

	No Binaries						Binaries					
	$Z = 0.016$		$Z = 0.008$		$Z = 0.004$		$Z = 0.016$		$Z = 0.008$		$Z = 0.004$	
$(m - M)_0$	⟨age⟩	$\langle M_e \rangle$	⟨age⟩	$\langle M_e \rangle$	⟨age⟩	$\langle M_e \rangle$	⟨age⟩	$\langle M_e \rangle$	⟨age⟩	$\langle M_e \rangle$	⟨age⟩	$\langle M_e \rangle$
						NGC 1866						
18.1.....	1.6 ± 0.3	4.3 ± 0.3	1.8 ± 0.5	4.0 ± 0.5	1.8 ± 0.7	3.9 ± 0.5	1.5 ± 0.2	4.1 ± 0.2	2.1 ± 0.2	3.8 ± 0.2	2.0 ± 0.5	3.7 ± 0.4
18.5.....	1.2 ± 0.2	4.8 ± 0.3	1.4 ± 0.4	4.4 ± 0.7	1.6 ± 0.7	4.2 ± 0.7	1.4 ± 0.2	4.5 ± 0.2	1.6 ± 0.2	4.2 ± 0.2	1.7 ± 0.5	4.1 ± 0.5
18.9.....	1.0 ± 0.2	5.2 ± 0.4	1.1 ± 0.4	4.9 ± 0.8	1.2 ± 0.6	4.7 ± 0.8	1.1 ± 0.1	4.9 ± 0.2	1.3 ± 0.3	4.6 ± 0.4	1.4 ± 0.4	4.5 ± 0.6
						NGC 2031						
18.1.....	1.5 ± 0.2	4.4 ± 0.3	1.8 ± 0.4	4.0 ± 0.4	1.8 ± 0.7	3.9 ± 0.5	1.5 ± 0.2	4.2 ± 0.2	2.0 ± 0.1	3.8 ± 0.1	2.0 ± 0.5	3.7 ± 0.4
18.5.....	1.2 ± 0.2	4.8 ± 0.4	1.4 ± 0.4	4.5 ± 0.5	1.4 ± 0.5	4.3 ± 0.6	1.3 ± 0.2	4.6 ± 0.2	1.6 ± 0.1	4.2 ± 0.2	1.7 ± 0.5	4.1 ± 0.5
18.9.....	1.0 ± 0.2	5.2 ± 0.5	1.1 ± 0.3	5.0 ± 0.7	1.1 ± 0.4	4.8 ± 0.8	1.1 ± 0.1	4.9 ± 0.2	1.3 ± 0.2	4.6 ± 0.3	1.2 ± 0.6	4.7 ± 0.8

[a] Ages are in units of 10^8 yr; masses are in solar units.

case, these stars may be blue stragglers of the sort discussed by Eggen & Iben (1988).

5. DISCUSSION

Having derived estimates of the pulsational and evolutionary masses of the Cepheids in NGC 1866 and NGC 2031 in § 3 and 4, we can now derive the distances of both clusters as a function of metallicity. The basic technique is illustrated in Figure 8 using NGC 1866 as an example and assuming $Z = 0.008$. The hatched region corresponds to the range of distance moduli where $M_{\rm puls} = M_{\rm evol}$; the vertical bar in Figure 8 indicates our best estimate of the distance modulus determined this way. This procedure was repeated for all other metallicities for the old (eq. [1]) and new (eqs. [2] and [3]) MPLC relations; the results are tabulated in Table 7. It is apparent that as the abundance decreases, so does the corresponding distance modulus. It is also evident that the results for both clusters are virtually identical and almost insensitive to the adopted MPLC relation. In Figure 9 we have plotted the average variation of the distance moduli of the two clusters as a function of $Z_1 \equiv \log (Z/0.016)$ based on the results from the MPLC relations given in equations (2) and (3). The average slope of these relations is $\Delta(m - M)_0/\Delta Z_1 = 0.69$.

What are the implications of this result? First, the ME method is only moderately sensitive to abundance: an uncertainty of a factor of 2 in Z_1 corresponds to a formal uncertainty of only 0.2 mag in the derived distance modulus. With regard to NGC 1866 and NGC 2031 in particular, we derive distance moduli of 18.51 ± 0.21 and 18.32 ± 0.20, respectively, assuming the abundances derived from the broad-band photometry of the Cepheids themselves (see § 2) and the MPLC relations of equations (2) and (3). These relative moduli are in general agreement with the tilted-disk model of the LMC proposed by Caldwell & Coulson (1986) which predicts that NGC

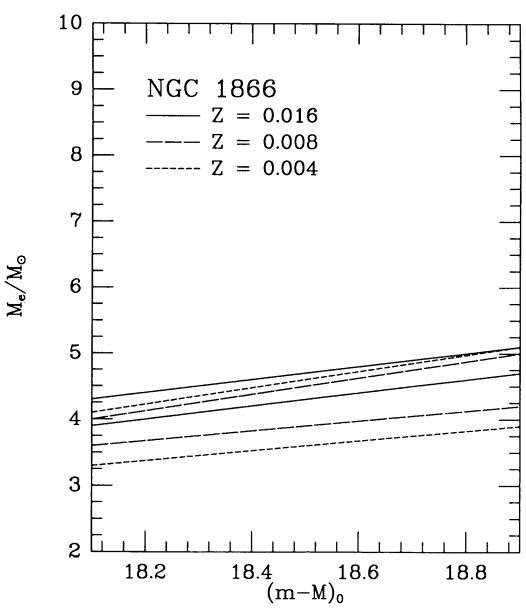

FIG. 7a

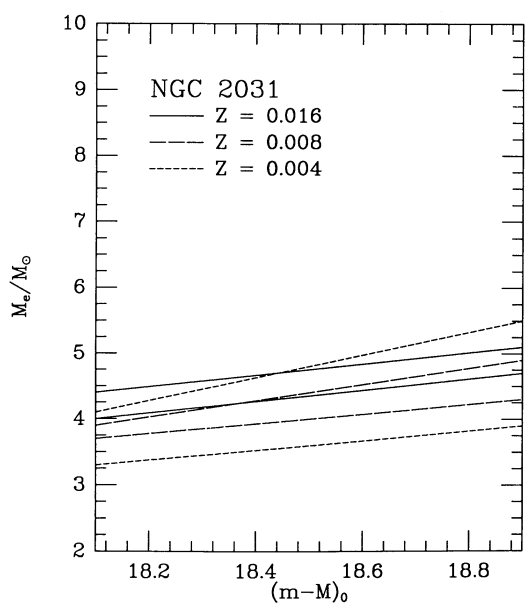

FIG. 7b

FIG. 7.—(*a*) Variation of the evolutionary mass of the Cepheids in NGC 1866 as a function of metallicity and assumed true distance modulus. (*b*) Same, for NGC 2031.

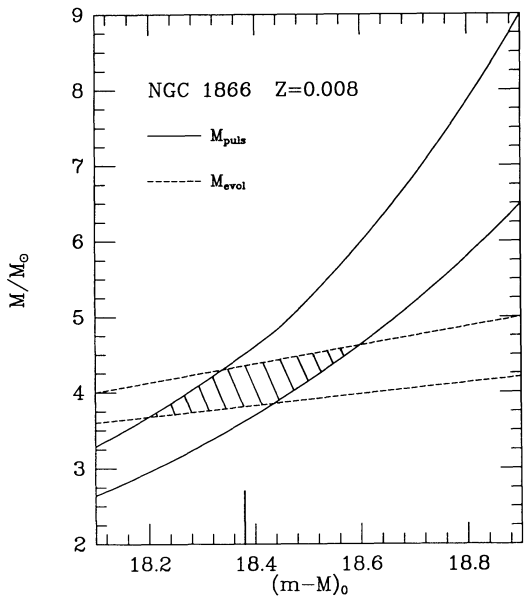

FIG. 8.—Run of pulsational and evolutionary masses of the Cepheids in NGC 1866 as a function of the distance modulus and assumed metallicity ($Z = 0.008$). The hatched region represents where the evolutionary masses equal the pulsational masses. The vertical bar shows the estimated true distance modulus (approximately the baricenter of the highlighted region).

2031 is 0.06 mag closer than NGC 1866. Of course, the errors are sufficiently large that the results could also be taken as evidence that the clusters are at the *same* distance. These distance moduli for NGC 1866 and NGC 2031 are consistent with the result for NGC 2157 based on the same method (Paper I), and with other independent recent estimates of the LMC distance modulus (Feast & Walker 1987; Walker 1988; Panagia et al. 1991). The present results also confirm the primary conclusion of Paper I that the Cepheid mass discrepancy can be eliminated using the Padova overshoot models and transformations in a manner consistent with independent distance estimates for the LMC. More generally, these studies demonstrate that the sensitivity of the ME method on metallicity is not so large that the precision of the derived distance moduli are

TABLE 7

DISTANCE MODULI, CEPHEID MASSES, AND AGES OF NGC 1866 AND NGC 2031[a]

Cluster	Z	$(m - M)_0$	$\langle M_{Ceph} \rangle$	$\langle$age$\rangle$
MPLC of Equation (1)				
NGC 1866.....	0.016	18.54 ± 0.11	4.5 ± 0.3	1.4 ± 0.2
	0.008	18.35 ± 0.14	4.1 ± 0.3	1.7 ± 0.3
	0.004	18.11 ± 0.10	3.6 ± 0.5	2.1 ± 0.4
NGC 2031.....	0.016	18.57 ± 0.13	4.6 ± 0.3	1.3 ± 0.2
	0.008	18.36 ± 0.11	4.1 ± 0.4	1.7 ± 0.3
	0.004	18.13 ± 0.14	3.8 ± 0.5	1.9 ± 0.4
MPLC of Equations (2) and (3)				
NGC 1866.....	0.016	18.57 ± 0.12	4.6 ± 0.3	1.3 ± 0.2
	0.008	18.38 ± 0.12	4.1 ± 0.4	1.7 ± 0.3
	0.004	18.16 ± 0.16	3.8 ± 0.5	1.9 ± 0.4
NGC 2031.....	0.016	18.60 ± 0.15	4.6 ± 0.3	1.3 ± 0.2
	0.008	18.40 ± 0.15	4.1 ± 0.4	1.7 ± 0.3
	0.004	18.18 ± 0.20	3.8 ± 0.5	1.9 ± 0.4

[a] Masses in solar units; ages in units of 10^8 yr.

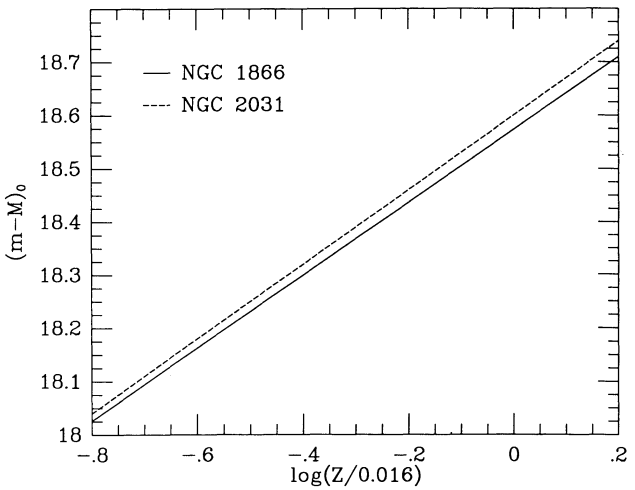

FIG. 9.—Variation of distance modulus with heavy-metal abundance, Z, for the ME method applied to NGC 1866 and NGC 2031.

compromised by "normal" uncertainties in the abundances of young clusters. Nevertheless, better abundance estimates for these clusters would be particularly helpful; it is clear from Figure 9 and Table 7 that for abundance estimates precise to ±0.15 dex or better, the primary source of uncertainty in the distances determined in this manner arises from the dispersion of the masses of the individual Cepheids in a given cluster.

The shortcomings of our analysis should also be emphasized. First, the values of the distance moduli derived for NGC 1866 and NGC 2031 are only as reliable as the evolutionary and pulsational models used in this study. For example, the debate regarding the necessity of convective overshoot and the suitability of present methods of accounting for such overshoot continues to rage (Renzini 1987; Zahn 1991; Stothers 1991; Stothers & Chin 1992; Paper I; Chiosi et al. 1993a). Moreover, these models incorporate different color-temperature transformations which lead to quite different moduli using the ME method for a given set of evolutionary models. However, the (mild) overshoot models used in this paper and in Paper I do resolve the Cepheid mass discrepancy problem for NGC 1866, NGC 2031 (this study) and NGC 2157 (Paper I) *for an LMC distance modulus consistent with other independent estimates.* From Paper I it is apparent that semi-convection models and/or the use of the "Yale" color-temperature conversion result in distance moduli from 0.25 to 0.5 mag larger than derived here. This implies that the models we have employed in this study may well be on the right track.

Of more concern is the recent report (Iglesias & Rogers 1991a, b; Rogers & Iglesias 1992) of significant changes in the radiative opacities at intermediate temperatures ($\sim 2 \times 10^5$ K). Simon (1982) and Andreasen (1988) noted that opacity changes in just this temperature range have potentially significant effects on Cepheid pulsational models. The models used in this paper are based on the older Los Alamos opacity tables of Huebner et al. (1977; see also Chiosi et al. 1993b for more details about the inclusion of the molecular opacities) and it is conceivable that the new opacities may change our conclusions significantly.

Although it is difficult to estimate the magnitude of the effect of the new opacities in general without calculating a complete new grid of models (these are in progress), some of the effects can be described from preliminary calculations. In Figure 10,

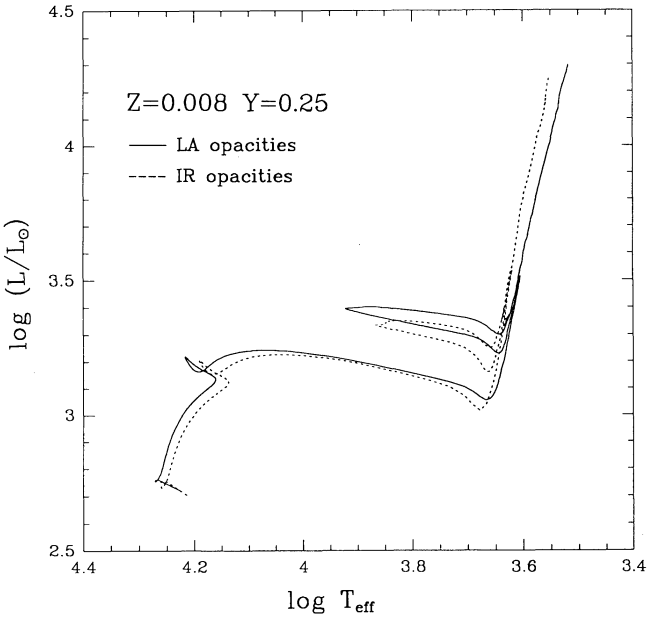

FIG. 10.—Two evolutionary tracks for 5 $M_\odot$ models based on overshoot models with $\Lambda = 0.5$. The solid line corresponds to the model using the Los Alamos opacities of Huebner et al. (1977); the dashed line corresponds to a model using the Iglesias & Rogers (1991a, b) and Rogers & Iglesias (1992) opacities.

we show two tracks for 5 $M_\odot$ overshoot models with an overshoot scale length of 0.5 pressure scale heights and $Z = 0.008$. The solid line in Figure 10 corresponds to a model based on the older Los Alamos opacities (hereafter the LA model), while the dashed line was computed using the newer opacities (hereafter the IR model). It is apparent that the blue loop of the IR model is about 0.1 lower in log L compared to the LA model. This implies the mass must be increased by 6.9% using the slope of the mass-luminosity relation adopted by Chiosi et al. (1993b). Because the luminosity difference between the IR and LA models is not large, the choice of the ML relation is not critical for this discussion. With regard to the pulsational masses, P. Antonello (1992, private communication) estimates an increase of 4% in the fundamental period for models incorporating the new opacities at a luminosity similar to that of the blue loops of the 5 $M_\odot$ tracks shown in Figure 10. Based on equation (2), this translates into a decrease in the mass (at a given color and luminosity) of 6%. These results imply that distance moduli obtained using the ME method and models incorporating the new opacities would be at most 0.1 mag *larger* for both NGC 1866 and NGC 2031. Consequently., the new opacities would not eliminate the ability of mild overshoot models to remove the evolutionary/pulsational Cepheid mass discrepancy. It will obviously be of great interest to repeat our analysis when fully consistent sets of intermediate-mass evolutionary and pulsational models using the new Livermore opacities become available.

6. SUMMARY AND CONCLUSIONS

In this paper, we have used the mild overshoot Padova stellar evolutionary models of Alongi et al. (1993) and the pulsational models of Chiosi et al. (1993b) to estimate the distances to the rich LMC clusters NGC 1866 and NGC 2031. The basis of our analysis is the requirement that the evolutionary and pulsational masses of the Cepheids in these clusters be equal. This approach—which we refer to as the "mass-equivalency," or ME, method—was successfully used to derive an estimate of the distance to the young LMC cluster NGC 2157 (Paper I) that is consistent with other independent distance determinations for the LMC. An important goal of the present paper was to investigate the sensitivity of the ME method on abundance.

The two primary conclusions of this study are as follows:

1. The true distance moduli of NGC 1866 and NGC 2031 are 18.51 ± 0.21 and 18.32 ± 0.20, respectively. The errors reflect (1) the range in pulsational and evolutionary masses of the Cepheids in each cluster, and (2) the large uncertainty (0.3 dex) of the abundances of each cluster. As in the case of NGC 2157, these distance estimates are comparable to recent independent distance determinations for the LMC, implying that the models used in this study effectively eliminate the evolutionary/pulsational mass discrepancy for classical Cepheids.

2. For Cepheids in the mass range corresponding to those found in NGC 1866 and NGC 2031 (4–5 $M_\odot$), the metallicity sensitivity of the distance moduli derived with the ME method is $\Delta(m - M)_0/\Delta Z_1 = 0.69$, where $Z_1 \equiv \log (Z/0.016)$. This implies that cluster abundance determinations accurate to 0.15 dex will be suitable to fix the cluster distances to $\pm 5\%$. At present, the abundance estimates for NGC 1866 and NGC 2031 are based on broad-band photometry of their Cepheids. However, both clusters (as well as other LMC clusters containing Cepheids) are rich in late-type supergiants suitable for much more precise spectroscopic abundance determinations.

There are numerous LMC clusters that contain Cepheids (Mateo 1993; Welch 1992); thus, the ME method can be used not only to precisely determine the distance to the LMC, but also its geometry along our line-of-sight as well. However, some fundamental issues remain to be thoroughly addressed before we can conclude the ME distances are systematically accurate. One important issue concerns the reliability of the zero-point of the distance scale implicit in our analysis. We plan to check this by comparing the evolutionary models used in this study with existing photometry of well-suited nearby clusters such as the Hyades, Pleiades, and Praesepe. In addition, the effects of the new Livermore opacities must be investigated carefully. We have argued in § 5 that the new opacities are unlikely to alter the relevant models to such an extent that the distances determined in this paper will change by more than 20%, and probably by considerably less. However, to tune the method at the 5% level, it is clearly necessary to adopt the most precise model parameters possible. In future applications of this method using other LMC clusters, we plan to investigate the effects of the new opacities in detail.

This study was supported by the Italian Ministry of University and Scientific and Technological Research (MURST), the National Council of Research (CNR-GNA), and the Italian Space Agency (ASI). M. M. acknowledges the support by NASA through grant HF-1007.01-90A awarded by the Space Science Telescope Institute, which is operated by the Association of Universities for Research in Astronomy, Inc., for NASA under contract NAS 5-26555.

REFERENCES

Alongi, M., Bertelli, G., Bressan, A., Chiosi, C., Fagotto, F., Greggio, L., & Nasi, E. 1993, A&AS, 97, 851
Andreasen, G. K. 1988, A&A, 201, 72
Becker, S. A., & Mathews, S. J. 1983, ApJ, 270, 155
Bessell, M. S., Brett, J. M., Scholz, M., & Wood, P. R. 1989, A&AS, 77, 1
Bertelli, G., Betto, F., Bressan, A., Chiosi, C., Nasi, E., & Vallenari, A. 1990, A&AS, 85, 845
Caldwell, J. A. R., & Coulson, I. M. 1985, MNRAS, 212, 879
———. 1986, MNRAS, 218, 223
Cardelli, J. A., Clayton, G. C., & Mathis, J. S. 1989, ApJ, 345, 245
Carney, B. W., Janes, K. A., & Flower, P. J. 1985, AJ, 90, 1196
Castellani, V., Chieffi, A., & Straniero, F. A. 1989, ApJS, 74, 463
Chiosi, C. 1991, in Confrontation between Stellar Pulsation and Evolution, ed. C. Cacciari & G. Clementini (ASP Conf. Ser., 11), 258
Chiosi, C., Bertelli, G., & Bressan, A. 1993a, ARA&A, 30, 235
Chiosi, C., Bertelli, G., Bressan, A., Wood, P. R., & Mateo, M. 1992, ApJ, 385, 205, (Paper I)
Chiosi, C., Bertelli, G., Meylan, G., & Ortolani, S. 1989a, A&AS, 78, 89
———. 1989b, A&A, 219, 167
Chiosi, C., Wood, P. R., & Capitanio, N. 1993b, ApJS, 86, 541
Da Costa, G. S. 1991, in The Magellanic Clouds, ed. R. Haynes & D. Milne (Dordrecht: Reidel), 183
Dean, J. F., Warren, P. R., & Cousins, A. W. J. 1978, MNRAS, 183, 569
Eggen, O. J., & Iben, I., Jr. 1988, AJ, 96, 635
Fagotto, F. 1990, Ph.D. thesis, Univ. Padova
Feast, M. W. 1988, in The World of Galaxies, ed. H. G. Corwin & L. Bottinelli (NY: Springer), 118
———. 1989, in The World of Galaxies, ed. H. G. Corwin & L. Bottinelli (NY: Springer), 118
Feast, M. W., & Walker, A. R. 1987, ARA&A, 25, 345
Fernie, J. D. 1990, ApJ, 354, 295
Green, E. M., Bessell, M. S., Demarque, P., King, C. R., & Peters, W. L. 1987, The Revised Yale Isochrones and Luminosity Functions (New Haven: Yale Univ. Obs.)
Huebner, W. F., Mertz, A. L., Magee, N. H. Jr., & Argo, M. F. 1977, Astrophysical Opacity Library Los Alamos, no. 6760-M
Iben, I., Jr., & Tuggle, R. S. 1972a, ApJ, 173, 135
———. 1972b, ApJ, 178, 441
———. 1975, ApJ, 197, 39
Iglesias, C. A., & Rogers, F. J. 1991a, ApJ, 371, 408
———. 1991b, ApJ, 371, L73
Lattanzio, J. C. 1991, ApJS, 76, 215
Maeder, A., & Meynet, G. 1988, A&AS, 76, 411
Mateo, M. 1993, PASP, 104, 824
Mateo, M., Olszewski, E. W., & Madore, B. F. 1990, ApJ, 353, L11
———. 1991, in Confrontation between Stellar Pulsation and Evolution, ed. C. Cacciari & G. Clementini (ASP Conf. Ser., 11), 214
Mateo, M., Olszewski, E., & Welch, D. 1993, in preparation
Olszewski, E. W., Schommer, R. A., Suntzeff, N. B., & Harris, H. C. 1991, AJ, 101, 515
Panagia, N., Gilmozzi, R., Macchetto, F., Adorf, H. M., & Kirshner, R. P. 1991, ApJ, 380, L23
Reitermann, A., Baschek, B., Stahl, O., & Wolf, B. 1990, A&A, 234, 109
Renzini, A. 1987, A&A, 188, 49
Rogers, F. J., & Iglesias, C. A. 1992, ApJ, 402, 361
Russell, S. C., & Bessell, M. S. 1989, ApJS, 70, 865
Russell, S. C., & Dopita, M. A. 1990, ApJS, 74, 93
Simon, N. R. 1982, ApJ, 260, L87
Stothers, R. B. 1991, ApJ, 383, 820
Stothers, R. B., & Chin, C. W. 1991, ApJ, 374, 288
———. 1992, ApJ, 390, 136
Vallenari, A. V., Chiosi, C., Bertelli, G., Meylan, G., & Ortolani, S. 1993, AJ, in press
Walker, A. 1987, MNRAS, 225, 627
———. 1988, in Extragalactic Distance Scale, ed. S. van den Bergh & C. J. Pritchett (ASP Conf. Ser., 4), 89
Welch, D. L. 1992, in Pulsating Variable Stars,
Welch, D. L., Mateo, M., Côté, P., Fischer, P., & Madore, B. F. 1991, AJ, 101, 490
Zahn, J. P. 1991, A&A, 252, 179